JACS
JOURNAL OF THE AMERICAN CHEMICAL SOCIETY
pubs.acs.org/JACS
Communication

An Open-Shell Functionalization of Inorganic Benzene

Sabrina Grenda,* Nicolas Claiser, Antonio Barbon, Frédéric Guégan, Bérangère Toury, and Dominique Luneau*

Cite This: J. Am. Chem. Soc. 2024, 146, 32906−32911
Read Online
ACCESS | Metrics & More | Article Recommendations | Supporting Information

ABSTRACT: A borazine derivative functionalized by nitroxide free radicals, *N*,*N*′,*N*″-(tris(4-Bromophenyl))-*B*,*B*′,*B*″-tris((2,6-dimethyl-4-(*N*-*tert*-butyl-*N*-oxyamino)phenyl) borazine (**TriBNit**), was synthesized as a milestone of open-shell inorganic benzene. The crystal structure determined from X-ray diffraction on a single crystal ascertains the grafting of three nitroxide radicals. The temperature dependence of the magnetic susceptibility evidences weak intramolecular antiferromagnetic interactions between the radicals with strong intermolecular antiferromagnetic interactions between two nitroxide moieties of two neighboring molecules. EPR spectroscopy at 80 K on a frozen glassy solution evidences the coexistence of $S = 1/2$ and $S = 3/2$ ground-spin state species. This is ascribed to the nitroxide radicals having different orientations with respect to the borazine core giving rise either to antiferromagnetic interaction with a low ground-spin state $S = 1/2$ or to ferromagnetic interaction with a high ground-spin state $S = 3/2$ as supported by theoretical data. At room temperature, because of nitroxide mobility, the EPR spectrum is averaged to a ground-spin state $S = 1/2$.

Open-shell molecules are an active research topic due to their promise in the field of molecule-based magnets, spintronic and quantum computing.[1−4] Here, we report the first example of an open-shell borazine. The six-member ring borazine core ($B_3N_3H_6$) with alternating B and N atoms and the B═N bond isoelectronic to the C═C one is known as the "inorganic benzene".[5−11] Nevertheless, the electronic properties of borazine demark from those of benzene due to the significant difference of boron and nitrogen electronegativities.[12] Though it has long been questioned, it is now well-established that borazine has a much lower aromaticity with the π-electron charge density mainly located on nitrogen atoms. This is supported by many theoretical studies[13] and a recent high-resolution X-ray diffraction study showing accumulation of the electron density at the nitrogen positions.[14]

Borazine ($B_3N_3H_6$) is extremely sensitive to moisture and can readily decompose into boric acid and ammonia.[15] Protection from hydrolysis is achieved through functionalization by bulky groups on the boron atoms,[16−19] among which is the industrial use of borazine and functionalized derivatives as a precursor of hexagonal boron nitride ceramic (h-BN) that is isoelectronic to graphite but white and an electrical insulator.[20,21] Recently, borazine derivatives deserve most interest for doping graphene with hybrid boron carbon nitride (BCN) fragments for optoelectronic and semiconductor properties,[22,23] but also as precursors for BN-doped polymers for their promising applications for gas storage and separation applications.[24,25]

As part of our investigations on nitroxide radicals as precursors of molecule-based magnets[26−28] and on borazine as a precursor of boron nitride and borophene,[29,30] we were interested to explore how much borazine could couple nitroxide radicals comparatively with other reported π-conjugated systems based on benzene,[31] s-triazine,[31,32] and s-triazine[32,33] and trioxytriphenylamine[34] cores. Moreover, reported DFT calculations have predicted the borazine core to be a better spin coupler, as compared to benzene.[35] This prompted us to design stable nitroxide-functionalized borazines, and we describe herein the synthesis and characterization of *N*,*N*′,*N*″-(tris(4-Bromophenyl))-*B*,*B*′,*B*″-tris((2,6-dimethyl-4-(*N*-*tert*-butyl-*N*-oxyamino)phenyl)borazine, referred to hereafter as **TriBNit** (**5**), where the functionalization is on the boron atoms.

B,*B*′,*B*″-Trichloro-*N*,*N*′,*N*″-tri(4-bromophenyl)borazine (**1**) and the O-silylated hydroxylamine **2** were first prepared with slight modifications of reported protocols.[18,31,36,37] **1** was chosen because bromine facilitates characterization by mass spectrometry and weighing while opening the way to further substitutions on the nitrogen atoms. First **2** was lithiated with an excess of *tert*-butyllithium and then coupled with 1/3 equiv of **1** to afford the protected functionalized borazine **3**. This was reacted with tetrabutylammonium fluoride (TBAF) in THF for desilylation to give compound **4**. **TriBNit 5** was finally obtained after oxidation of **4** with $NaIO_4$ in a biphasic system of water and dichloromethane and further purification by silica column chromatography (Scheme 1).

TriBNit 5 shows remarkable stability to hydrolysis as is illustrated by the oxidation done in aqueous media. The crystal structures of precursors **2a** and **2** and triradical **TriBNit 5** were determined by X-ray diffraction on single crystals grown by

Received: August 6, 2024
Revised: November 13, 2024
Accepted: November 14, 2024
Published: November 20, 2024

Scheme 1. Synthetic Pathway for the Preparation of a Nitroxide-Bearing Borazine

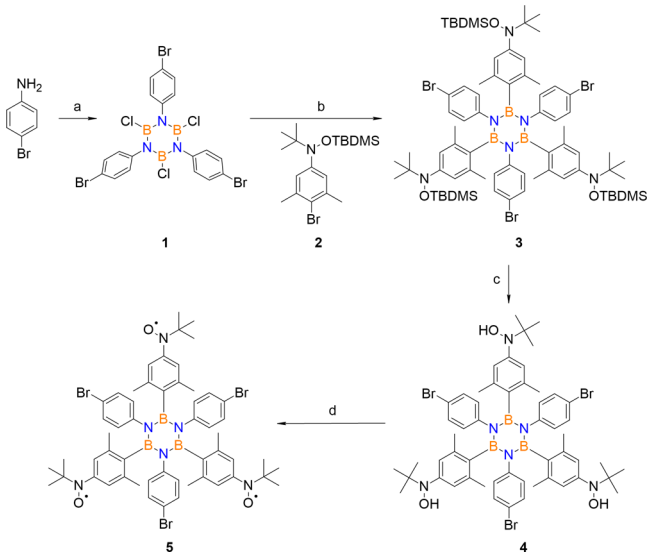

[a]BCl_3/Toluene (1 M), reflux 24 h, 70% yield. [a′]TBDMSCl, Imidazome, DMF, 60 °C for 16 h, 53% yield. [b]Toluene, ^{t}BuLi/hexane (1.7 M), −78 °C to RT, 40% yield. [c]TBAF/THF (1 M), reflux 48 h, 27% yield. [d]CH_2Cl_2/$NaIO_4$ aq, 22% yield.

slow evaporation of solution of the compounds in acetone (**2a**), methanol (**2**) and dichloromethane (**5**). Crystallographic data are listed in Table S1. Crystallographic data of precursors **2a** and **2** and views of their asymmetric units in Figure S11 are provided for additional information. **TriBNit 5** crystallizes in the triclinic $P\bar{1}$ space group (Figure 1). The asymmetric unit comprises one complete molecule of **5** with one-half molecule of cocrystallized dichloromethane. As expected, the molecule

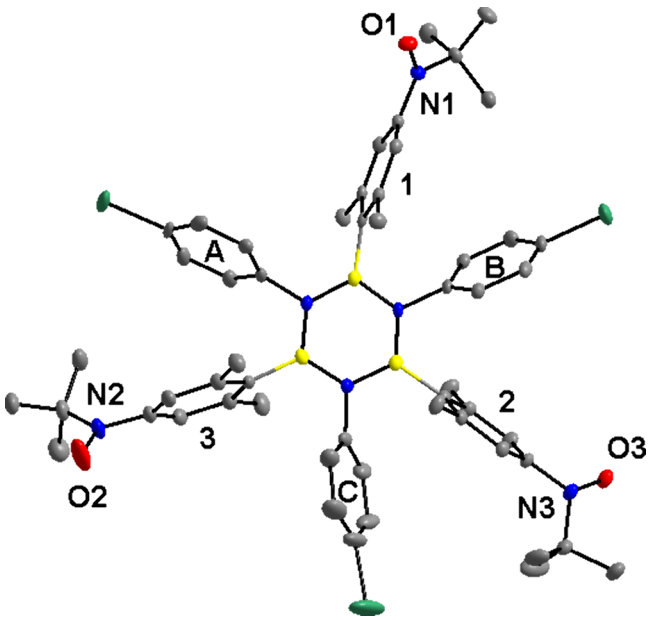

Figure 1. View of molecule **TriBNit 5** from the crystal structure represented with thermal ellipsoid plot at a 50% level. Hydrogen atoms and atoms from dichloromethane are omitted for clarity. Atoms are colored as follows: B in yellow; N in blue; O in red; Br in green; C in gray.

shows a quasi-orthogonal arrangement of the aryl moieties due to steric hindrance. Tilted angles are reported in Table S2.

The three *para* substituted 4-bromophenyl groups labeled A, B, and C (Figure 1) are tilted by 67.99°, 67.18°and 68.04° respectively to the B_3N_3-core. The tilt angles are even larger for *B*-aryls groups carrying the nitroxide moieties, labeled 1, 2, 3 (Figure 1), with values of 80.47°, 77.39° and 80.59°. These values are higher than those reported for trinitroxide radicals with benzene,[31] s-triazine,[31,32] and s-triazine[32,33] with tilted angles of aryl groups in the range of 5°−19.5°. Regarding torsion angles between the O−N−C_{sp2} plane and the aryl group to which it is attached, N1−O1 and N2−O2 make a torsion angle in the same direction of 38.82° and 42.78° respectively. The third nitroxide group N3−O3 is oriented in the opposite direction with dihedral angle 37.87°. The angles are slightly larger than 5°−37.5° reported in the literature.[31−33,38] The N−O bond lengths are between 1.279 and 1.286 Å and are similar to values reported on CSD for *para*-phenylene and *para*-aryl substituted nitroxide groups, which are found between 1.26 and 1.31 Å (Figure S11). This definitively rules out any hydroxylamine form and confirms the presence of three nitroxide radicals in compound **5**. Through space intramolecular distances between the oxygen atoms of the nitroxide groups are 14.080 Å (O1—O2), 12.913 Å (O1—O3) and 14.151 Å (O2—O3).

In the crystal, **TriBNit 5** makes 2D sheets separated by 11.89 Å and parallel to the (120) Miller plane with the borazine ring in plane (Figure S13). Within the 2D sheets, molecules **5** are like paired putting one of their NO groups at short intermolecular distances 2.376 Å (O3α—N3α') in a head to tail arrangement. The other NO groups show greater spacing with 4.290 and 7.769 Å found for O1α—N1α' and O2α—N2α', respectively. The dichloromethane molecule is not involved in significant contact with the NO groups but exhibits a π-halogen interaction with a 4-bromoaniline fragment. ($d_{C-Cl—\pi}$ = 4.386 Å) (Figure S14)

Room temperature continuous wave EPR (cw-EPR) spectrum of degassed toluene solution of **5** shows a typical seven-line hyperfine structure centered at g = 2.0068 (Figure 2a), accounting for an intramolecular spin exchange interaction J larger (in absolute value) than J = −0.02 cm^{-1} ca. between two nitroxide pairs while the third pair should have a much smaller interaction. No half-field resonance corresponding to $\Delta m_s = \pm 2$ was detected near 1720 G ascribed to the too small dipolar coupling between the nitroxide moieties: they are situated far apart as revealed by the crystallographic structure. In order to determine the ground-state spin, we performed EPR nutation experiments. For on-resonance spins, in the absence of spin relaxation, the nutation is a precessional motion of the equilibrium macroscopic magnetization about the rotating microwave field B_1.[39] The nutation frequency depends on the magnetic microwave field B_1 and on the S-value of the species.[40,41] Nutation experiments can therefore be used to differentiate the different spin states in a molecule by plotting the echo intensity of a 2-pulse experiment as a function of the magnetic microwave field B_1.[40] For more details, see SI section 5.2. A solution of nitroxide radical TEMPO in toluene at equal concentrations was the reference. At room temperature, the nutation profile of **TriBNit 5** and TEMPO are nearly equal suggesting a spin state of S = 1/2, and a J-value smaller than k_BT (200 cm^{-1} ca. at room temperature), which do not contradict cw-EPR measurements, suggesting an interaction larger (in absolute value) than −0.02

https://doi.org/10.1021/jacs.4c10736
J. Am. Chem. Soc. 2024, 146, 32906−32911

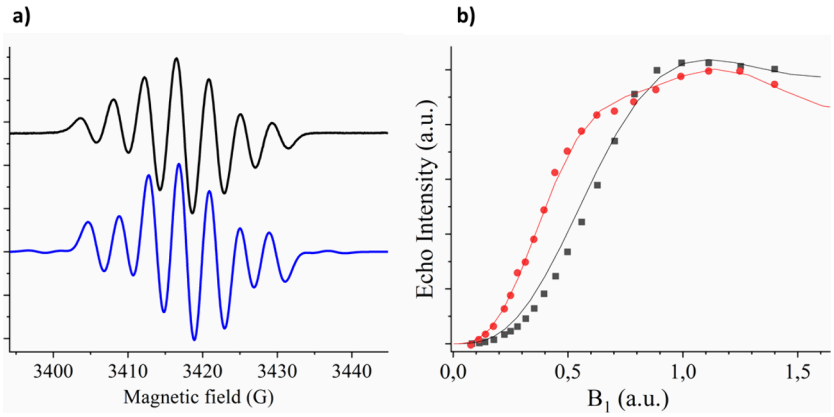

Figure 2. (a) X-band room-temperature cw-EPR spectra of **TriBNit 5** in a 0.1 mM solution of toluene (black) together with its simulation $J > 500$ MHz (0.02 cm^{-1} ca). (b) Two-pulse electron spin echo nutation as a function of the microwave B_1 intensity for TEMPO (black squares) and **5** in frozen toluene solution (0.1 mM) at 80 K. The lines are the relative simulations (the model is described in the SI).

cm^{-1} ca. At 80 K, in frozen solution, the cw-EPR spectrum of 5 was much less informative with a nearly structureless bell-shape (Figure S12), while the echo nutation experiment gives a complex profile rather different from that of the TEMPO (Figure 2b). Fitting of the echo nutation spectrum with a model based on the solution of the Bloch equations[42] and taking into an account spin diffusion mechanisms of type T_1[40] highlighted the coexistence of an $S = 1/2$ spin state (73%) and an $S = 3/2$ spin state (27%). It is likely that these two components result from different conformations of the nitroxide moieties on the molecule coexisting in the frozen state, causing the interactions between the radicals to be either antiferromagnetic ($S = 1/2$) or ferromagnetic ($S = 3/2$). At room temperature, the free motion of the nitroxide radicals in the fluid solution modulates the spin−spin interaction so that the ground state is averaged as an $S = 1/2$ ground-state spin (Figure S15).

Magnetic properties of **TriBNit 5** were investigated on a powder sample check by X-ray diffraction (Figure S19). At 300 K the product of the magnetic susceptibility with temperature χT (~0.91 emu·K·mol^{-1}) is slightly lower than the expected value (~1.125 emu·K·mol^{-1} assuming $g = 2$) for three magnetically independent nitroxide radicals with spin $S = 1/2$ (Figure 3). Upon cooling, χT decreases continuously to 0.71 emu·K·mol^{-1} at 80 K. From there, it remains almost constant down to 30 K and then decreases abruptly to reach 0.14 emu·K·mol^{-1} at 3 K.

This behavior suggests the presence of antiferromagnetic (AF) interactions in the crystalline state. This was fitted using the PHI program[43] and considering a six-spin model which holds for intermolecular exchange coupling in between two paired molecules **5** (Figure 4). The best fit evidence the presence of weak intramolecular antiferromagnetic interactions with $J_{1-2} = J_{1-3} = -5.4$ cm^{-1} and $J_{2-3} = -0.4$ cm^{-1}, dominated by a strong intermolecular antiferromagnetic interaction between two nitroxide moieties with $J_{1-1} = -214$ cm^{-1}. Then, the plateau of χT below 80 K is consistent with two independent spin $S = 1/2$ per molecule. These results are consistent with analysis of the crystal structure that shows short intermolecular distances of 2.376 Å between the N−O groups of two neighboring molecules in a head-to-tail fashion which favors the strong antiferromagnetic coupling.[44]

Ab initio calculations were additionally conducted on one isolated molecule **TriBNit 5** taken from the X-ray structure.

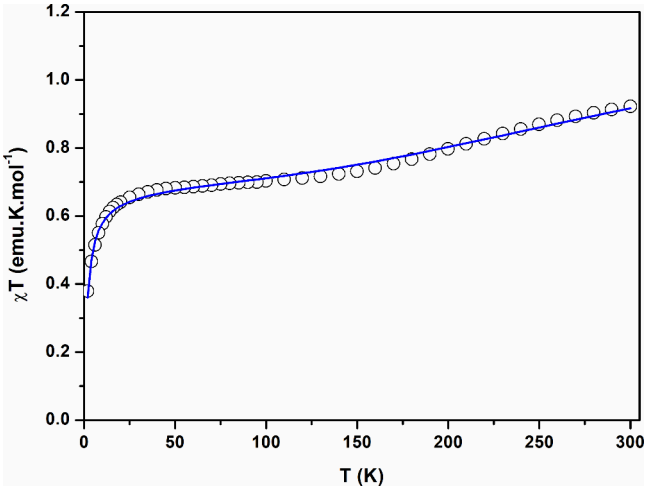

Figure 3. Temperature dependence of the χT observed for **5** measured at 0.1. The solid blue line is simulated the PHI program.[43]

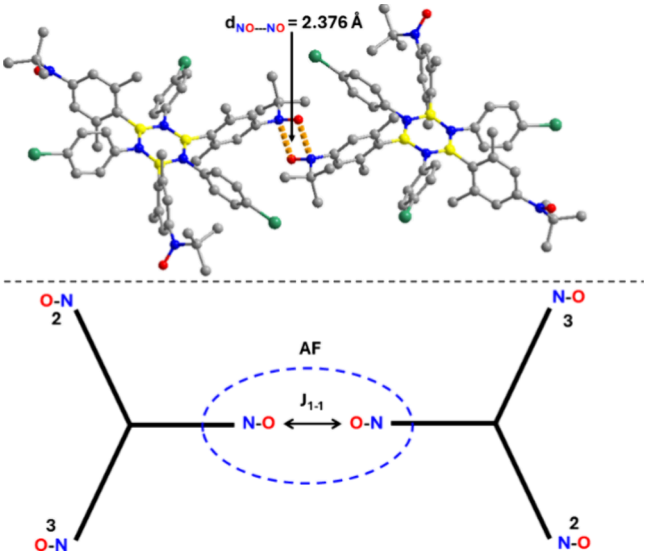

Figure 4. Scheme of two paired molecules **5** holding for a six-spin model (bottom) with a view of the nitroxide groups leading to the intermolecular antiferromagnetic coupling exchange (top).

https://doi.org/10.1021/jacs.4c10736
J. Am. Chem. Soc. 2024, 146, 32906−32911

Successive Domain-Based Local Pair Natural Orbital State-Averaged N-Electron Valence Perturbation Theory at second order (DLPNO-SA-NEVPT2) calculations were undertaken,[45−47] averaging over two doublet and one quartet states, and using DFT (B3LYP/def2-TZVP) Quasi-Restricted Orbitals for the quartet state as a guess (Figure 21S). The size of the active space was gradually increased from the minimal active space (3 electrons in 3 orbitals) to a 17 electrons, 11 orbitals active space. Throughout the calculations, at the CASSCF level almost no intramolecular coupling is found from calculations, the energy gap between the degenerate doublets and the quartet being only 0.1 cm^{-1}. Including the NEVPT2 correction leads to small stabilization of the quartet state, resulting eventually in an energy splitting with the two doublets of +1.1 cm^{-1} and +1.2 cm^{-1} for the DLPNO-SA-NEVPT2(17,11).

This very small energy splitting thus indicates the borazine core is not providing here any support to spin coupling, at variance with predicted DFT calculations.[35] It also suggests that the sign of the coupling may be altered by conformational changes providing explanation to the observed "mixture of states" in EPR experiments in frozen solutions, but also by crystal packing and Madelung field.[48]

In summary, this paper reports the first example of an open-shell borazine synthesized after boron functionalization by three nitroxide radicals, as supported by the crystal structure of the solid-phase crystallized from a dichloromethane solution. Study of the temperature dependence of the magnetic susceptibility of this crystalline material evidences intra- and intermolecular antiferromagnetic interactions both contributing to an $S = 1/2$ ground-state spin. At 80 K when solution is frozen, the EPR evidences a mixture of $S = 1/2$ and $S = 3/2$ spin states. In agreement with calculations, this reflects that, at 80 K, molecules are frozen with different conformations of the nitroxide radicals relative to the borazine core, giving rise either to antiferromagnetic or ferromagnetic interaction between the three nitroxide radicals to give, respectively, a doublet or a quartet ground-state spin. This work contributes to a better understanding of how the borazine core can couple spins. Further works dealing with functionalization on nitrogen atoms and on both boron and nitrogen atoms are in progress, as well as trials to crystallize the solid-phase exhibiting a quartet ground state as inspired by EPR on frozen solution.

■ ASSOCIATED CONTENT

Supporting Information

The Supporting Information is available free of charge at https://pubs.acs.org/doi/10.1021/jacs.4c10736.

Experimental details on synthesis, characterization of compound **1**, **2a**, **2**, **3**, **4**, and **5**, copies of NMR spectra and mass spectroscopy spectra, Fitting protocol and model of the echo nutation experiment, powder X-ray diffraction, X-ray crystal structure determination and magnetic studies complemented by, powder XRD patterns and additional Tables and Figures for crystal structures and magnetism; The authors have cited additional references within the Supporting Information[49−58] (PDF)

Accession Codes

Deposition Numbers 2314106, 2314126, and 2365689 contain the supplementary crystallographic data for this paper. These data can be obtained free of charge via the joint Cambridge Crystallographic Data Centre (CCDC) and Fachinformationszentrum Karlsruhe Access Structures service.

■ AUTHOR INFORMATION

Corresponding Authors

Sabrina Grenda − *Laboratoire des Multimatériaux et Interfaces (UMR 5615), Université Claude Bernard Lyon 1, 69100 Villeurbanne, France;* orcid.org/0000-0003-2484-725X; Email: sabrina.grenda@univ-lyon1.fr

Dominique Luneau − *Laboratoire des Multimatériaux et Interfaces (UMR 5615), Université Claude Bernard Lyon 1, 69100 Villeurbanne, France;* orcid.org/0000-0002-1831-7693; Email: dominique.luneau@univ-lyon1.fr

Authors

Nicolas Claiser − *Laboratoire de Cristallographie, Resonance Magnétique et Modélisation (UMR 7030), Université de Lorraine, 54506 Vandoeuvre-lès-Nancy CEDEX, France;* orcid.org/0000-0002-4469-7220

Antonio Barbon − *Department of Chemical Sciences, University of Padova, I-35131 Padova, Italy;* orcid.org/0000-0002-2009-5874

Frédéric Guégan − *Institut de Chimie des Milieux et Matériaux de Poitiers (UMR 7285), Université de Poitiers, 86000 Poitiers, France;* orcid.org/0000-0002-4932-8643

Bérangère Toury − *Laboratoire des Multimatériaux et Interfaces (UMR 5615), Université Claude Bernard Lyon 1, 69100 Villeurbanne, France;* orcid.org/0000-0001-5889-0796

Complete contact information is available at: https://pubs.acs.org/10.1021/jacs.4c10736

Notes

The authors declare no competing financial interest.

■ ACKNOWLEDGMENTS

This work was supported by the LABEX iMUST of the University of Lyon (ANR-10-LABX-0064), created within the "Plan France 2030" set up by the French government and managed by the French National Research Agency (ANR). DL and AB thank the Arqus European University Alliance for mobility support to SG to carry collaborative EPR study at Università degli Studi di Padova (Italy). This support was granted by the European Commission under the project 612247-EPP-1-2019-1-ES-EPPKA2-EUR-UNIV. Région Auvergne-Rhône-Alpes and its programme "Amorçage Europe" for financial support (No. 23 007040 01−40890).

■ REFERENCES

(1) Zaytseva, E.; Timofeev, I.; Krumkacheva, O.; Parkhomenko, D.; Mazhukin, D.; Sato, K.; Matsuoka, H.; Takui, T.; Bagryanskaya, E. EPR and DEER Characterization of New Mixed Weakly Coupled Nitroxide Triradicals for Molecular Three-Spin Qubits. *Appl. Magn. Reson.* **2019**, *50* (8), 967−976.

(2) Kubo, T. Syntheses and Properties of Open-Shell π-Conjugated Molecules. *Bull. Chem. Soc. Jpn.* **2021**, *94* (9), 2235−2244.

(3) Li, L.; Prindle, C. R.; Shi, W. Z.; Nuckolls, C.; Venkataraman, L. Radical Single-Molecule Junctions. *J. Am. Chem. Soc.* **2023**, *145*, 18182.

(4) Suzuki, S. *Recent Progress in Stable High-Spin Molecules Based on Nitroxide Radicals* **2015**, 323.

(5) Fasano, F.; Dosso, J.; Bezzu, C. G.; Carta, M.; Kerff, F.; Demitri, N.; Su, B. L.; Bonifazi, D. BN-Doped Metal-Organic Frameworks:

Tailoring 2D and 3D Porous Architectures through Molecular Editing of Borazines. *Chem.—Eur. J.* **2021**, *27* (12), 4124−4133.
(6) Lorenzo-García, M. M.; Bonifazi, D. Renaissance of an Old Topic: From Borazines to BN-doped Nanographenes. *Chimia* **2017**, *71* (9), 550−557.
(7) Marwitz, A. J. V.; Matus, M. H.; Zakharov, L. N.; Dixon, D. A.; Liu, S. Y. A Hybrid Organic/Inorganic Benzene. *Angew. Chem., Int. Ed.* **2009**, *48* (5), 973−977.
(8) Neogi, I.; Szpilman, A. M. Synthesis and Reactions of Borazines. *Synthesis-Stuttgart* **2022**, *54* (08), 1877−1907.
(9) Ota, K.; Kinjo, R. A Neutral and Aromatic Boron-Rich Inorganic Benzene. *Angew. Chem., Int. Ed.* **2020**, *59* (16), 6572−6575.
(10) Oubaha, H.; Demitri, N.; Rault-Berthelot, J.; Dubois, P.; Coulembier, O.; Bonifazi, D. Photoactive Boron-Nitrogen-Carbon Hybrids: From Azo-borazines to Polymeric Materials. *J. Org. Chem.* **2019**, *84* (14), 9101−9116.
(11) Marchionni, D.; Basak, S.; Khodadadi, A. N.; Marrocchi, A.; Vaccaro, L. Synthesis and Applications of Organic Borazine Materials. *Adv. Funct. Mater.* **2023**, DOI: 10.1002/adfm.202303635.
(12) Kalemos, A. The nature of the chemical bond in borazine (B3N3H6), boroxine (B3O3H3), carborazine (B2N2C2H6), and related species. *Int. J. Quantum Chem.* **2018**, DOI: 10.1002/qua.25650.
(13) Baez-Grez, R.; Pino-Rios, R. The hidden aromaticity in borazine. *RSC Adv.* **2022**, *12* (13), 7906−7910.
(14) Merino-Garcia, M. D.; Soriano-Agueda, L. A.; Guzman-Hernandez, J. D.; Martinez-Otero, D.; Landeros Rivera, B.; Cortes-Guzman, F.; Barquera-Lozada, J. E.; Jancik, V. Benzene and Borazine, so Different, yet so Similar: Insight from Experimental Charge Density Analysis. *Inorg. Chem.* **2022**, *61* (18), 6785−6798.
(15) Yoshizaki, T.; Watanabe, H.; Nakagawa, T. Kinetics and Mechanisms of Hydrolysis of Borazine Derivatives in Aqueous Dioxane. *Inorg. Chem.* **1968**, *7* (3), 422.
(16) Nagasawa, K. Borazines Stable to Hydrolysis. *Inorg. Chem.* **1966**, *5* (3), 442.
(17) Wakamiya, A.; Ide, T.; Yamaguchi, S. Toward p-conjugated molecule bundles: Synthesis of a series of B,B′,B″-trianthryl-N,N′,N″-triarylborazines and the bundle effects on their properties. *J. Am. Chem. Soc.* **2005**, *127* (42), 14859−14866.
(18) Kervyn, S.; Fenwick, O.; Di Stasio, F.; Shin, Y. S.; Wouters, J.; Accorsi, G.; Osella, S.; Beljonne, D.; Cacialli, F.; Bonifazi, D. Polymorphism, Fluorescence, and Optoelectronic Properties of a Borazine Derivative. *Chem.—Eur. J.* **2013**, *19* (24), 7771−7779.
(19) Bonifazi, D.; Fasano, F.; Lorenzo-Garcia, M. M.; Marinelli, D.; Oubaha, H.; Tasseroul, J. Boron-nitrogen doped carbon scaffolding: organic chemistry, self-assembly and materials applications of borazine and its derivatives. *Chem. Commun.* **2015**, *51* (83), 15222−15236.
(20) Paine, R. T.; Narula, C. K. Synthetic routes to boron-nitride. *Chem. rev.* **1990**, *90* (1), 73−91.
(21) Miele, P.; Bernard, S.; Cornu, D.; Toury, B. Recent developments in polymer-derived ceramic fibers (PDCFs): Preparation, properties and applications - A review. *Soft Mater.* **2007**, *4* (2−4), 249−286.
(22) Sánchez-Sánchez, C.; Brüller, S.; Sachdev, H.; Müllen, K.; Krieg, M.; Bettinger, H. F.; Nicolaï, A.; Meunier, V.; Talirz, L.; Fasel, R.; et al. On-Surface Synthesis of BN-Substituted Heteroaromatic Networks. *ACS Nano* **2015**, *9* (9), 9228−9235.
(23) Caputo, L.; Nguyen, V. H.; Charlier, J. C. First-principles study of the structural and electronic properties of BN-ring doped graphene. *Phys. Rev. Mater.* **2022**, DOI: 10.1103/PhysRevMaterials.6.114001.
(24) Riensch, N. A.; Deniz, A.; Kühl, S.; Müller, L.; Adams, A.; Pich, A.; Helten, H. Borazine-based inorganic-organic hybrid cyclomatrix microspheres by silicon/boron exchange precipitation polycondensation. *Polym. Chem.* **2017**, *8* (35), 5264−5268.
(25) Jackson, K. T.; Rabbani, M. G.; Reich, T. E.; El-Kaderi, H. M. Synthesis of highly porous borazine-linked polymers and their application to H_2, CO_2, and CH_4 storage. *Polym. Chem.* **2011**, *2* (12), 2775−2777.
(26) Grenda, S.; Beau, M.; Luneau, D. Synthesis, Crystal Structure and Magnetic Properties of a Trinuclear Copper(II) Complex Based on P-Cresol-Substituted Bis(α-Nitronyl Nitroxide) Biradical. *Molecules* **2022**, *27* (10), 3218.
(27) Luneau, D. Coordination Chemistry of Nitronyl Nitroxide Radicals Has Memory. *Eur. J. Inorg. Chem.* **2020**, *2020* (7), 597−604.
(28) Mathevet, F.; Luneau, D. Interpenetrated 3D polymeric metal-radical networks built from a tetranitroxide radical and bis-(hexafluoroacethylacetonato) manganese(II). *J. Am. Chem. Soc.* **2001**, *123* (30), 7465−7466.
(29) Matsoso, B.; Hao, W. J.; Li, Y. D.; Vuillet-a-Ciles, V.; Garnier, V.; Steyer, P.; Toury, B.; Marichy, C.; Journet, C. Synthesis of hexagonal boron nitride 2D layers using polymer derived ceramics route and derivatives. *J. Phys. Mater.* **2020**, *3* (3), 034002.
(30) Mignon, P.; Allouche, A. R.; Innis, N. R.; Bousige, C. Neural Network Approach for a Rapid Prediction of Metal-Supported Borophene Properties. *J. Am. Chem. Soc.* **2023**, *145* (50), 27857−27866.
(31) Kanno, F.; Inoue, K.; Koga, N.; Iwamura, H. Persistent 1,3,5-benzenetriyltris(N-tert-buty nitroxide) and its analogs with quartet ground-states - Intramolecular triangular exchange coupling among 3 nitroxide radical centers. *J. Phys. Chem. A* **1993**, *97* (50), 13267−13272.
(32) Hayami, S.; Inoue, K. Structure and magnetic property of the organic triradical with triazine skeleton;: 2,4,6-Tris{*p*-*N*-*oxy*-*N*-*tert*-butylamino)phenyl}triazine. *Chem. Lett.* **1999**, *28* (7), 545−546.
(33) Lahti, P. M.; Liao, Y.; Julier, M.; Palacio, F. s-triazine as an exchange linker in organic high-spin molecules. *Synth. Met.* **2001**, *122* (3), 485−493.
(34) Suzuki, S.; Nagata, A.; Kuratsu, M.; Kozaki, M.; Tanaka, R.; Shiomi, D.; Sugisaki, K.; Toyota, K.; Sato, K.; Takui, T.; et al. Trinitroxide-Trioxytriphenylamine: Spin-State Conversion from Trir-adical Doublet to Diradical Cation Triplet by Oxidative Modulation of a p-Conjugated System. *Angew. Chem., Int. Ed.* **2012**, *51* (13), 3193−3197.
(35) Bhattacharya, D.; Shil, S.; Misra, A.; Bytautas, L.; Klein, D. J. Borazine: spin blocker or not? *Phys. Chem. Chem. Phys.* **2015**, *17* (21), 14223−14237.
(36) Allaoud, S.; Conte, S.; Fenet, B.; Frange, B.; Robert, F.; Secheresse, F.; Karim, A. H-1 and C-13 NMR-studies of Eta-6-benzo-bonded (Boron-Nirogen Heteroarene) tricarbonylchromium complexes and related eta-6-phenyl-bonded (B,B′,B″-trimethyl-N,N′,N″-Triarylborazine)-Tricarbonylchromium complexes-crystallographic structure of boron-nitrogen Heteroarene. *J. Organomet. Chem.* **1994**, *469* (1), 59−68.
(37) Itoh, T.; Matsuda, K.; Iwamura, H.; Hori, K. Tris[p-(N-oxyl-N-tert-butylamino)phenyl]amine, -methyl, and -borane Have Doublet, Triplet, and Doublet Ground States, Respectively. *J. Am. Chem. Soc.* **2000**, *122* (11), 2567−2576.
(38) Suzuki, S.; Okada, K. Magnetic Properties of Multiradicals Based on Triarylamine Radical Cations. In *Organic Redox Systems: Synthesis, Properties, and Applications*; Nishinaga, T., Ed.; Wiley, 2015.
(39) Barbon, A.; Rusetsky, G. A.; Linarello, S.; Strzelczyk, R.; Fedaruk, R. Peculiarities in Rabi oscillations for fast-relaxing electron spins. *J. Magn. Reson.* **2024**, *368*, 107781.
(40) Schweiger, A.; Jeschke, G. *Principles of Pulse Electron Paramagnetic Resonance*; Oxford University Press, 2001. DOI: 10.1093/oso/9780198506348.001.0001.
(41) Fedaruk, R.; Strzelczyk, R.; Rusetsky, G. A.; Barbon, A.; Majchrzycki, L.; Augustyniak-Jablokow, M. A. Continuous-wave and pulsed EPR studies of glass-like carbon with high spin concentration: Evidence for triplet states. *Carbon* **2023**, *213*, 118270.
(42) Grivet, J. P. Simulation of Magnetic-Resonance Experiments. *Am. J. Phys.* **1993**, *61* (12), 1133−1139.
(43) Chilton, N. F.; Anderson, R. P.; Turner, L. D.; Soncini, A.; Murray, K. S. PHI: A powerful new program for the analysis of anisotropic monomeric and exchange-coupled polynuclear d- and f-block complexes. *J. Comput. Chem.* **2013**, *34* (13), 1164−1175.

(44) Alies, F.; Luneau, D.; Laugier, J.; Rey, P. Ullman Nitroxide Biradicals Revisited - Structural and Magnetic-Properties. *J. Phys. Chem. A* **1993**, *97* (12), 2922−2925.
(45) Dhara, D.; Endres, L.; Krummenacher, I.; Arrowsmith, M.; Dewhurst, R. D.; Engels, B.; Bertermann, R.; Finze, M.; Demeshko, S.; Meyer, F. Synthesis and Reactivity of a Dialane-Bridged Diradical. *Angew. Chem., Int. Ed.* **2024**, DOI: 10.1002/anie.202401052.
(46) Guo, Y.; Sivalingam, K.; Valeev, E. F.; Neese, F. SparseMaps-A systematic infrastructure for reduced-scaling electronic structure methods. III. Linear-scaling multireference domain-based pair natural orbital N-electron valence perturbation theory. *J. Chem. Phys.* **2016**, DOI: 10.1063/1.4942769.
(47) Neese, F. Software update: The ORCA program system-Version 5.0. *Wiley Interdiscip. Rev. Comput. Mol. Sci.* **2022**, DOI: 10.1002/wcms.1606.
(48) Lepetit, M. B.; Suaud, N.; Gelle, A.; Robert, V. Environment effects on effective magnetic exchange integrals and local spectroscopy of extended strongly correlated systems. *J. Chem. Phys.* **2003**, *118* (9), 3966−3973.
(49) Emsley, P.; Cowtan, K. *Coot*: model-building tools for molecular graphics. *Acta Cryst. D* **2004**, *60*, 2126−2132.
(50) Fegy, K.; Luneau, D.; Ohm, T.; Paulsen, C.; Rey, P. Two-dimensional nitroxide-based molecular magnetic materials. *Angew. Chem., Int. Ed.* **1998**, *37* (9), 1270−1273.
(51) Hirel, C.; Vostrikova, K. E.; Pecaut, J.; Ovcharenko, V. I.; Rey, P. Nitronyl and imino nitroxides: Improvement of Ullman's procedure and report on a new efficient synthetic route. *Chem.—Eur. J.* **2001**, *7* (9), 2007−2014.
(52) Kabsch, W. XDS. *Acta Cryst. D* **2010**, *66*, 125−132.
(53) Kahn, O. *Molecular Magnetism*; VCH: New York, 1993.
(54) Kovalevskiy, O.; Nicholls, R. A.; Long, F.; Carlon, A.; Murshudov, G. N. Overview of refinement procedures within *REFMAC5*: utilizing data from different sources. *Acta Cryst. D* **2018**, *74*, 215−227.
(55) Lannes, A.; Suffren, Y.; Tommasino, J. B.; Chiriac, R.; Toche, F.; Khrouz, L.; Molton, F.; Duboc, C.; Kieffer, I.; Hazemann, J. L.; et al. Room Temperature Magnetic Switchability Assisted by Hysteretic Valence Tautomerism in a Layered Two-Dimensional Manganese Radical Coordination Framework. *J. Am. Chem. Soc.* **2016**, *138* (50), 16493−16501.
(56) Lecourt, C.; Izumi, Y.; Khrouz, L.; Toche, F.; Chiriac, R.; Bélanger-Desmarais, N.; Reber, C.; Fabelo, O.; Inoue, K.; Desroches, C.; et al. Thermally-induced Hysteretic Valence Tautomeric Conversions in Solid State via Two-step Labile Electron Transfers in Manganese-Nitronyl Nitroxide 2D-Frameworks. *Dalton Trans.* **2020**, *49*, 15646−15662.
(57) Lecourt, C.; Izumi, Y.; Maryunina, K.; Inoue, K.; Belanger-Desmarais, N.; Reber, C.; Desroches, C.; Luneau, D. Hypersensitive pressure-dependence of the conversion temperature of hysteretic valence tautomeric manganese-nitronyl nitroxide radical 2D-frameworks. *Chem. Commun.* **2021**, *57* (19), 2376−2379.
(58) Luneau, D.; Borta, A.; Chumakov, Y.; Jacquot, J.-F.; Jeanneau, E.; Lescop, C.; Rey, P. Molecular magnets based on two-dimensional Mn(II)-nitronyl nitroxide frameworks in layered structures. *Inorg. Chim. Acta* **2008**, *361* (12−13), 3669−3676.